Contrast discrimination in noise

Gordon E. Legge

University of Minnesota, Minneapolis, Minnesota 55455

Daniel Kersten

Brown University, Providence, Rhode Island 02912

Arthur E. Burgess

University of British Columbia, Vancouver, British Columbia V5C 1M9, Canada

Received January 6, 1986; accepted September 2, 1986

Even the highest contrast sensitivities that humans can achieve for the detection of targets on uniform fields fall far short of ideal values. Recent theoretical formulations have attributed departures from ideal performance to two factors—the existence of internal noise within the observer and suboptimal stimulus information sampling by the observer. It has been postulated that the contributions of these two factors can be evaluated separately by measuring contrast-detection thresholds as a function of the level of externally added visual noise. We wished to determine whether a similar analysis could be applied to contrast discrimination and whether variation of the increment threshold with pedestal contrast is due to changes in internal noise or sampling efficiency. We measured contrast-increment thresholds as a function of noise spectral density for near-threshold and suprathreshold pedestal contrasts. The experiments were conducted separately for static and dynamic noise. Our findings indicate that the same formulation can be applied to contrast discrimination and that changes in the estimated values of internal noise, rather than changes in sampling efficiency, play the major role in determining properties of contrast discrimination. Implications for models of contrast coding in vision are discussed.

INTRODUCTION

The research reported here was conducted in two laboratories—one at the University of Minnesota (Minnesota) and the other at the University of British Columbia (UBC). At Minnesota, contrast discrimination was measured for 2-cycles/degree (c/deg) sine-wave gratings in two-dimensional dynamic visual noise. At UBC, contrast discrimination was measured for 13.6-arcmin-diameter disks in two-dimensional static noise. The details of apparatus and procedure differ somewhat, but the research questions are the same. We are therefore presenting our results in a single paper.

In a contrast-discrimination experiment, observers are required to distinguish between pairs of stimuli identical except for their contrasts C and $C + \Delta C$. The threshold value of ΔC is called the *contrast-increment threshold*. The value of C upon which it is superimposed is called the *pedestal contrast*. The relation between ΔC and C for a given target is called the *contrast-discrimination function* for that target.

Authors of recent studies[1–4] generally agree that the contrast-discrimination functions for many stimuli are dipper shaped. As pedestal contrast rises from zero, the increment threshold first declines. This facilitation effect occurs for pedestal contrasts near the contrast-detection threshold. For suprathreshold contrasts, ΔC rises with pedestal contrast. For many conditions, ΔC is related to C by a power law with an exponent near 0.6.[5,6] This general description applies to several classes of target.[5–9]

Why do contrast-increment thresholds change when pedestal contrast is varied? One way of dealing with this question is to compare an observer's performance with *ideal performance*. Recently there have been three similar treatments of visual performance that have taken this approach.[10–12] A real observer's deviation from ideal performance is characterized by two general factors, the level of *internal noise* and the *efficiency* with which the observer collects the available stimulus information. For targets added to uniform fields, the contrast thresholds of real observers greatly exceed ideal thresholds. *A priori*, there is no way of knowing whether this deviation from ideal performance is due to internal noise within the observer, to inefficient sampling of stimulus information by the observer, or to both. However, the effects of these two factors can be evaluated separately by measuring visual thresholds as a function of the level of *externally added visual noise*. The following paragraphs outline the approach in detail.

Let the luminance profile of the pedestal be $L_p(x, y, t)$ and the luminance profile of the signal-plus-pedestal be $L_{s+p}(x, y, t)$. We define the *signal function* S to be the difference of the luminance profiles, normalized by the mean luminance L_0,[13]

$$S(x, y, t) = [L_{s+p}(x, y, t) - L_p(x, y, t)]/L_0.$$

The *signal energy* is defined to be the integral over space and time of the squared signal function:

$$E = \iiint S^2(x, y, t)\mathrm{d}x\mathrm{d}y\mathrm{d}t.$$

If x and y are measured in degrees of arc and t in seconds, signal energy has units of (deg^2 sec). In several of the fig-

0740-3232/87/020391-14$02.00

ures, the units are $\mu(\text{deg}^2\ \text{sec})$, meaning 10^{-6} deg^2 sec. For stimuli of fixed size and duration, signal energy is proportional to the square of signal contrast. In the case of static viewing, the signal function has no time dependence, and signal energy has units of deg^2.

There have been several studies in which contrast thresholds were measured in the presence of visual noise. *Visual noise* is composed of random luminance samples in one or two spatial dimensions and/or time. It is characterized by its noise spectral density N. (Details of noise spectral density and noise bandwidth will be described in the Minnesota Method section.) In such experiments it has been shown that the signal energy of targets at threshold E_t is related to the noise spectral density N by a function of the form[11,15,16]

$$E_t = k(N + N_{eq}) = kN + kN_{eq}. \quad (1)$$

The slope k and the intercept N_{eq} are estimated from the data. Larger values of either of these parameters correspond to higher thresholds and hence poorer performance. These parameters are interpreted as two qualitatively different ways in which detection performance can be limited; N_{eq} is related to the level of internal noise and k to the efficiency with which the observer samples the available stimulus information.

A nonzero value of N_{eq} indicates that the observer behaves as if a constant, intrinsic noise is added to the external visual noise. N_{eq} is called the observer's equivalent noise. The term "equivalent noise" is used because N_{eq} is expressed in units of noise spectral density and can be regarded as equivalent to an irreducible source of noise added to the stimulus.[11] The noise may be associated with the transduction from stimulus to neural signal or may be related more directly to the decision process itself, e.g., variability of a decision criterion.[17]

The value of the constant k in Eq. (1) relates to a second kind of performance limitation. An ideal observer for whom intrinsic noise is zero will achieve a detectability d' equal to $\sqrt{(E/N)}$ for a target of signal energy E embedded in noise of spectral density N.[18] If we define an ideal observer's threshold by a criterion level of detectability d'_c, the relationship between threshold signal energy E_t and noise spectral density N will be

$$d'_c = \sqrt{(E_t/N)} \quad \text{or} \quad E_t = (d'_c)^2 N \text{ (ideal observer)}. \quad (2)$$

If humans were ideal, except for internal noise, the constant k in Eq. (1) would be equal to $(d'_c)^2$, as required by Eq. (2). Measured values of k for humans are higher than $(d'_c)^2$, however, revealing a second kind of inefficiency in performance. We define an observer's *sampling efficiency* J by the relation

$$J = (d'_c)^2/k. \quad (3)$$

Using this definition, Eq. (1) may be rewritten as

$$E_t = [(d'_c)^2/J](N + N_{eq}).$$

If we take the criterion level of detectability d'_c that determines threshold to be 1, we have

$$E_t = (1/J)(N + N_{eq}) \quad \text{(threshold criterion, } d' = 1). \quad (1a)$$

This means that, in a graph of threshold signal energy as a function of noise spectral density, the higher the slope is, the lower the sampling efficiency is.

The term "sampling efficiency" was introduced by Burgess *et al.*[12] and was discussed in detail by Burgess and Barlow.[19] Essentially the same concept is termed "calculation efficiency" by Pelli[11] and "central efficiency" by Barlow.[10]

Values of sampling efficiency lower than 1 reflect a failure by the observer to collect the available information optimally. The optimal strategy is one that maximizes the signal-to-noise ratio; in other words, it is a strategy in which the signal information is extracted while the effects of noise are kept at a minimum. When signal parameters are known in advance, the optimal strategy is implemented by weighting the stimulus, in both space and time, in proportion to the profile of the expected signal, i.e., cross correlation. If we think of the cross correlation as the convolution of the stimulus with some receptive-field profile, then a mismatch between receptive-field shape and signal shape would result in reduced sampling efficiency. If the receptive field is larger than the signal, all the signal information is collected, but extra noise is also collected, and the signal-to-noise ratio is suboptimal. If the receptive field is smaller than the signal, some signal information is lost, and the signal-to-noise ratio is again suboptimal. Incomplete spatial or temporal summation would also result in reduced sampling efficiencies.

Under some conditions, sampling efficiency can be very high. Burgess *et al.*[12] found a sampling efficiency of 70% for low-contrast-increment detection. The target was a Gaussian-windowed 2-cycle-wide 4.6-c/deg sine-wave grating. Efficiency was measured for static noise with unlimited viewing time. Sampling efficiency may be lower in dynamic noise. Kersten[20] found a sampling efficiency of 30% for the detection of a Gaussian-windowed 2-c/deg grating in spatially one-dimensional dynamic noise. Kersten measured efficiency as a function of the grating's width, that is, distance between the $1/e$ points of the Gaussian window. The maximum efficiency occurred for gratings about 1 cycle wide, with a rapid decrease in efficiency for gratings of greater width. In two other studies employing dynamic noise, Kersten and Barlow[21,22] found that sampling efficiencies did not exceed 30%.

The separate effects of equivalent noise and sampling efficiency are illustrated in Fig. 1. Threshold signal energy E_t is plotted as a function of noise spectral density, both in the same units. Threshold is defined by a criterion detectability of $d' = 1$. The curves represent particular cases of Eq. (1). The intercept on the vertical axis is signal energy at threshold in the absence of external noise. The horizontal intercept gives the negative of the equivalent noise, and the reciprocal of the slope is the sampling efficiency. For an ideal observer (dashed curve in the figure), the equivalent noise[23] is zero, and the sampling efficiency is 1.0. The ideal observer's threshold curve is determined by the equation, $E_t = N$. This is the best possible performance. By comparison, curves A and B are not ideal. Both have nonzero equivalent noise, although both have sampling efficiencies of 1.0. Curve C has an equivalent noise of 1.0, like curve A, but a sampling efficiency of only 0.5. Notice that the threshold energy in the absence of noise (vertical intercept) for curves B and C is twice that for curve A. This threshold elevation is

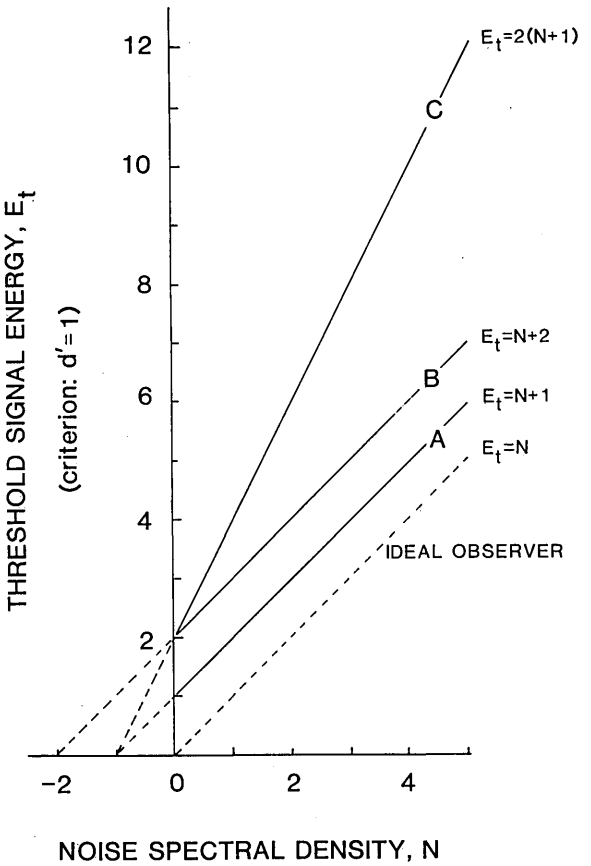

Fig. 1. Some special cases of the linear model of Eq. (1). Threshold signal energy is plotted as a function of noise spectral density, both in the same units. Threshold is defined by a criterion detectability of $d' = 1$. The ideal observer exhibits a sampling efficiency of 1 and an equivalent noise of zero. Curve A has a sampling efficiency of 1 and an equivalent noise of 1. Curve B has a sampling efficiency of 1 and an equivalent noise of 2. Curve C has a sampling efficiency of 0.5 and an equivalent noise of 1.

due to increased equivalent noise in the case of curve B and to reduced sampling efficiency in the case of curve C. Whether a change in equivalent noise or a change in sampling efficiency causes the threshold elevation cannot be determined simply by measuring thresholds in the absence of noise. However, as Fig. 1 shows, measurements with noise permit the distinction to be made.

Can an analysis like the one just described for contrast detection be applied to contrast discrimination? We must first ask whether Eq. (1) holds for the relationship between signal energy of a just-detectable contrast increment and noise spectral density. The work of Burgess *et al.*[12] suggests that it does, at least for a near-threshold pedestal. If so, we may then ask how equivalent noise and sampling efficiency change with pedestal contrast. Which of these factors is primarily responsible for the dip in the contrast-discrimination function for near-threshold pedestals, and which is responsible for the rise in increment thresholds for high-contrast pedestals?

Pelli[11] reported measurements of increment threshold versus pedestal contrast in the absence of noise and in the presence of two levels of external noise. He did not directly evaluate changes in equivalent noise or sampling efficiency. However, a rough analysis of Pelli's data indicates that changes in equivalent noise play a more important role in determining properties of the contrast-discrimination function than changes in sampling efficiency. For example, when detection and discrimination for a near-threshold pedestal were compared, sampling efficiency did not change by more than a factor of 1.5, whereas equivalent noise dropped by a factor of 4. On the other hand, for a pedestal with contrast 10 times threshold, sampling efficiency is still not much changed, whereas the equivalent noise has risen by a factor of 6. Note, however, that in a recent paper Pelli[24] has used a scaling principle to argue that these same data are consistent with invariant equivalent noise for subthreshold pedestals.

To assess the roles of equivalent noise and sampling efficiency in contrast discrimination, we measured contrast-increment thresholds in noise for several pedestal contrasts and noise spectral densities. Evidence cited earlier suggests that detection performance may be less efficient in dynamic than in static noise. It is possible that factors limiting performance may be different in these two cases. We therefore examined the effects of both forms of noise—dynamic noise at Minnesota and static noise at UBC.

Implications of our results for models of contrast discrimination will be taken up in the Discussion.

METHOD: UNIVERSITY OF MINNESOTA

Apparatus

The patterns were produced on the face of a Joyce Electronics cathode-ray-tube (CRT) display by Z-axis modulation.[25] The display had a P31 phosphor, an unmodulated luminance of 340 cd/m^2, and a dark surround. At the viewing distance of 228 cm, the screen subtended 7.5° horizontally by 4° vertically. The display was calibrated in both the horizontal and the vertical directions with a UDT 80X optometer with microphotometer attachment.

The signal luminance waveforms were synthesized digitally by an LSI-11/23 computer. In each 10-msec frame, the computer generated 600 pairs of voltage samples that were routed through two 12-bit digital-to-analog converters (DAC's). One DAC generated the signal and the other the pedestal. The output of each DAC was routed through a programmable decibel attenuator so that the contrasts of signal and pedestal could be controlled separately. The attenuators were also used to modulate the waveforms temporally. The attenuated waveforms were added and then multiplied by the output of a third DAC that served to modulate the patterns along the raster lines of the CRT. The third DAC was triggered by the raster synchronization pulse and produced 160 samples per raster line. The resulting waveform was then added to the noise.

The noise varied in time and two spatial dimensions. Binary pseudorandom noise was digitally synthesized by a 31-bit shift register with exclusive-or feedback[11,26] at a sample rate of 5 MHz. The noise voltage was passed through a high-bandwidth passive attenuator to set the noise level.

Stimuli

The luminance at a point x, y (in degrees relative to the fixation mark) at time t (milliseconds) is given by

$$L(x, y, t) = L_0[1 + m(x, y, t)q(x)],$$

where L_0 is the mean luminance. The term $q(x)$ is given by

$$q(x) = C \cos(2\pi fx)$$

for the pedestal and by

$$q(x) = (C + \Delta C)\cos(2\pi fx)$$

for the signal-plus-pedestal, where C and ΔC are the Michelson contrasts of the pedestal and signal. The spatial frequency f was always 2 c/deg. The modulating function $m(x, y, t)$ is given by the product of Gaussian functions horizontally, vertically, and temporally:

$$m(x, y, t) = \exp[-(x/s_x)^2 - (y/s_y)^2 - (t/s_t)^2],$$

where s_x, s_y, and s_t are the horizontal, vertical, and temporal space constants, respectively. The horizontal and vertical space constants were 0.5°. The time constant was 80 msec.

For Gaussian noise, the amplitudes of the samples have a Gaussian distribution. The bandwidth of the noise is determined by the spatial and temporal extents of the samples and the correlations, if any, between samples. In our experiments, the noise samples were uncorrelated. The *two-sided noise spectral density* N is defined to be the variance of the sampling distribution divided by the two-sided bandwidth, i.e., twice the one-sided bandwidth. Pelli[11] has pointed out that two-sided noise spectral densities are notationally convenient. Using the two-sided definition, the expression discussed in the Introduction for ideal detectability, $d' = \sqrt{(E/N)}$, is independent of the dimensionality of the noise. Using a one-sided definition, a more awkward expression results, $d' = \sqrt{(2^k E/N)}$, where the noise is k dimensional. In this paper, "noise spectral density" refers to "two-sided noise spectral density." When the noise has one temporal and two spatial dimensions, the units are $1/[(\text{c/deg})^2\text{Hz}] = \text{deg}^2$ sec. Accordingly, the units of noise spectral density and signal energy are the same.

The horizontal, vertical, and temporal dimensions of the uncorrelated noise samples were 0.0085 deg, 0.083 deg, and 0.01 sec, respectively.[27] The noise was turned on abruptly 160 msec before the maximum contrast was reached and turned off abruptly 160 msec later. The noise filled the screen both horizontally and vertically.

For each of the three pedestal contrasts—0, 0.01, and 0.25—increment thresholds were measured for four noise spectral densities. Noise spectral densities were computed by multiplying the squared rms noise contrast by the product of the sample sizes in the x, y, and t directions.[29] The relation between noise spectral density N and rms noise contrast C is $N = 7.06 \times 10^{-6}\ C_{\text{rms}}^2\ \text{deg}^2$ sec.

Procedures

Contrast-increment thresholds were obtained by using a two-alternative forced-choice version of the method of constant stimuli. For each pedestal contrast, three increment contrasts were used. Within each trial, one of these was chosen at random and added to the pedestal in one of the intervals. The intervals were separated by 600 msec, and each was marked by an auditory tone. A feedback tone indicated to the observer whether he or she was right.

Each of the resulting psychometric functions was based on 300 trials. Four of these functions were collected in one session, one for each of the four noise levels. These measurements were repeated in four successive sessions. In alternate sessions the noise levels were employed in ascending and descending order.

The raw data consisted of the number of trials and percentages correct for each of a set of three increment contrasts added to a given pedestal. Percentages were transformed to detectability d'.[30] The data were then fitted by functions of the form

$$d' = (C/C')^n. \tag{4}$$

C' is the contrast for which $d' = 1$ and is taken to be the threshold contrast. (It corresponds to the contrast associated with about 76% correct in forced choice.) n is a parameter representing the steepness of the psychometric function. Maximum-likelihood estimates were found for the parameters C' and n. Separate estimates of C' and n were obtained for each of the four repetitions of each psychometric function for each condition.

There were two observers, DR and MK, both naive about the details of the experiment. Subject DR is an emmetrope and subject MK a corrected myope. Viewing was binocular with natural pupils and with a fixation point at the center of the screen.

METHOD: UNIVERSITY OF BRITISH COLUMBIA

Apparatus

Patterns were produced on the face of a Tektronix 634 monochrome TV monitor. The monitor had a white P4 phosphor with unmodulated luminance of 150 cd/m^2 and a dark surround. At the viewing distance of 143 cm, the display subtended 3.6° horizontally by 4.5° vertically. Calibrations were conducted with a Tektronix J16 photometer and J6523 telephotometer attachment.

The patterns were created digitally by a PDP-11/34 computer and loaded into a Ramtek 9100 display system. The Ramtek generated a 256 (vertical) × 320 (horizontal) pixel display quantized to 256 gray levels per pixel. The nonlinear relation between monitor luminance and signal voltage was canceled by an inverse transformation loaded into a lookup table on the Ramtek's video output board. The pedestal and pedestal-plus-increment were created as independent digital images. The static, two-dimensional noise was generated off line by the UBC Computer Center's random-number generator and added to these digital images. The noise had a Gaussian probability density function, and the samples were uncorrelated. When required, the resulting digital waveforms were loaded into the Ramtek's memory for subsequent display.

Stimuli

The targets were disks of uniform luminance superimposed upon the 150-cd/m^2 background. The disks subtended 13.6 arcmin. (Actually, the targets were not exactly circular because of the discrete size of the individual pixels. However, the targets had a diameter of 16 pixels and were nearly circular.) The pedestal and pedestal-plus-increment were presented on the left- and the right-hand sides of the display in a spatial forced-choice paradigm. The pedestal had con-

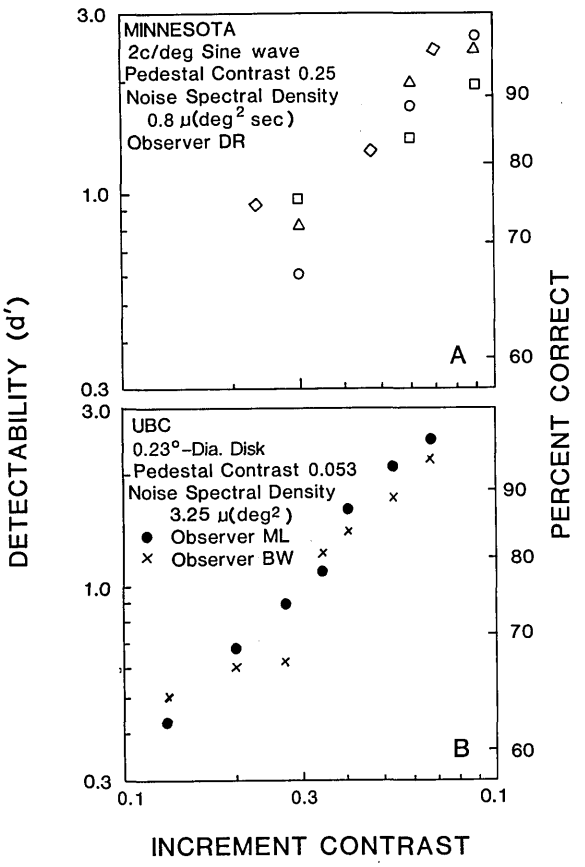

Fig. 2. Illustrative psychometric functions. Detectability (left-hand ordinate) and percent correct (right-hand ordinate) are plotted as a function of increment contrast for fixed values of pedestal contrast and noise spectral density. A, Dynamic noise (Minnesota): the four symbols show replications in four separate sessions for one observer. Each point is based on about 100 trials. B, Static noise (UBC): the two symbols show psychometric functions for two observers under identical conditions.

trast C and pedestal-plus-increment $C + \Delta C$. Here, contrast is defined to be $\Delta L/L_0$, where L_0 is the background luminance and ΔL is the change of luminance associated with the target.

Static noise was restricted to square patches, centered on the target disks, but of twice the diameter, i.e., 32 × 32 pixels. The two-sided vertical and horizontal bandwidths of the static noise were 74 c/deg. The targets and noise were turned on abruptly together and left on until the observer made a decision. For each of the five pedestal contrasts—0.053, 0.107, 0.21, 0.32, and 0.43—increment thresholds were obtained for five noise spectral densities—0, 0.203, 0.812, 1.83, and 3.25 $\mu(\text{deg}^2)$.[31]

Procedure

For a given pedestal contrast and noise spectral density, a fixed contrast increment was selected. A spatial two-alternative forced-choice procedure was used. In a trial, the pedestal was presented on one side of the screen, and the pedestal-plus-increment on the other, both embedded in noise. The observer was required to indicate on which side of the screen the increment was presented. The observer was free to look back and forth. Feedback was given about the outcome of the trial. Percent correct was obtained from a block of 400 such trials. Percent correct was converted to detectability d'.[30] Assuming a linear relationship between d' and increment contrast (see Fig. 2B), the value of increment contrast for which $d' = 1$ was calculated. This value was taken as the *threshold increment contrast*.

Two well-practiced but naive observers participated. Viewing was binocular with natural pupils.

RESULTS: UNIVERSITY OF MINNESOTA

The Minnesota results refer to discrimination of 2-c/deg sine-wave targets with Gaussian envelopes in space and time. Measurements were conducted in two-dimensional dynamic noise.

Figure 2A shows the four psychometric functions collected from subject DR for a pedestal contrast of 0.25 and noise spectral density of 0.8 $\mu(\text{deg}^2\ \text{sec})$. Detectability d' is plotted against increment contrast on a log–log scale. Corresponding values of percent correct are shown on the right-hand ordinate. The different symbols represent data collected in different sessions. Each set of data is based on approximately 300 trials. Thresholds and slopes were estimated from each set of data (see the Minnesota Method section). The threshold was the increment contrast for which $d' = 1$. Mean thresholds and slopes were then computed for the four sets of data. The same approach was used to estimate thresholds and slopes for all conditions.

As an aside, we consider the log–log slopes of the psychometric functions. These slopes have significance for models of detection and discrimination. Table 1 lists slopes for two observers, three pedestal contrasts, and four noise spectral densities. In all, the 24 estimates are based on 96 separate psychometric functions. According to the table, the slopes tend to be larger than 1 when the pedestal is low *and* the noise level is low. For example, for simple detection in the absence of noise, the slopes are slightly greater than 2. This result is consistent with previous findings (see, e.g., Foley and Legge[4]). However, for high noise *or* suprathreshold pedestals, the slopes cluster near 1. Kersten[20] found slopes near 1 for detection of 2-c/deg gratings in one-dimensional dynamic noise.

The analysis summarized by Eq. (1) and illustrated in Fig. 1 requires a linear relationship between threshold signal

Table 1. Mean Slopes of Psychometric Functions (Minnesota Data)[a]

Pedestal Contrast	Noise Spectral Density [$\mu(\text{deg}^2\ \text{sec})$]	Subject DR	Subject MK
0	0	2.06	2.13
	0.177	1.20	1.54
	0.8	1.49	1.04
	4.43	1.00	1.18
0.01	0	1.50	1.38
	0.011	1.28	1.56
	0.044	1.29	1.54
	0.177	1.12	0.86
0.25	0	1.11	0.95
	0.177	0.93	1.04
	0.8	0.97	1.00
	4.43	1.01	0.71

[a] The psychometric data were fitted by functions of the form $d' = (C/C')^n$. This table contains estimated values of n. Each estimate is the mean of four values, each obtained from a psychometric function.

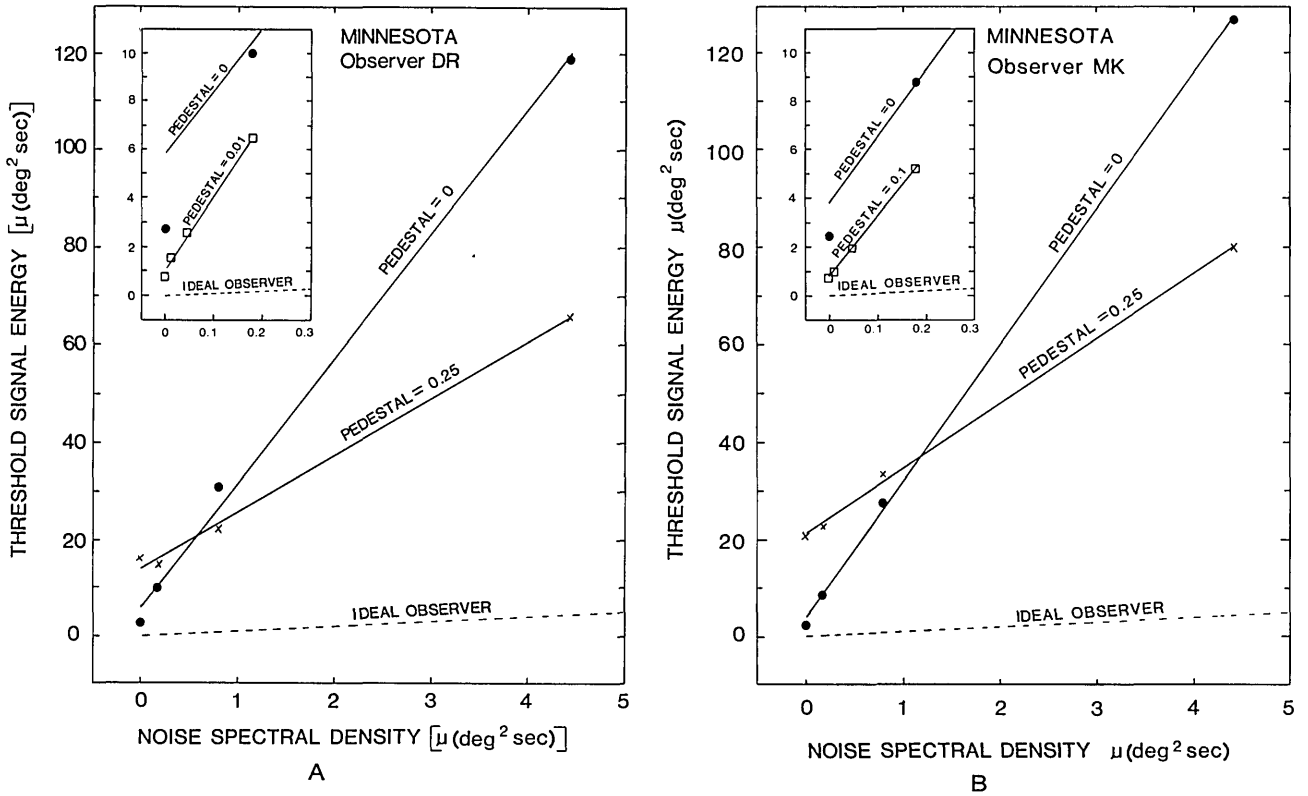

Fig. 3. Threshold signal energy as a function of noise spectral density in dynamic noise (Minnesota). The main graph compares data for pedestals having contrasts of zero and 0.25. The inset shows data for the 0.01-contrast pedestal and some of the data for the zero-contrast pedestal replotted from the main graph. Best-fitting straight lines (least-squares criterion) have been fitted to the three sets of data. The dashed line with slope 1.0 shows the performance of an ideal observer having a sampling efficiency of 1.0 and equivalent noise of zero. The relation between signal energy E and contrast C is $E = 0.0192C^2$ deg^2 sec. Accordingly, the 0.01- and 0.25-contrast pedestals have energies of 1.92 and 1200 μ(deg^2 sec), respectively. μ(deg^2 sec) means 10^{-6} deg^2 sec. A and B show data for two observers.

energy and noise spectral density, apart from the additive constant associated with equivalent noise. We began by asking whether a linear relationship provided a good fit to our discrimination data. For each pedestal, we tested the hypothesis that nonlinear terms would provide a significantly better fit than a linear regression (see Hays,[33] Sec. 16.4). In no case did the F test show a significant result, $p < 0.05$. We therefore conclude that the linear model [Eq. (1)] describes not only contrast detection but also contrast discrimination in noise. We can therefore examine the effects of pedestal contrast on the intercept and slope parameters, i.e., on equivalent noise and sampling efficiency.

In Fig. 3, mean threshold data are plotted for the two observers in the format of Fig. 1. The abscissa is noise spectral density, and the ordinate is threshold signal energy, both in units of μ(deg^2 sec). The dashed line with slope 1.0 in each panel represents the performance of an ideal observer. The three sets of data correspond to the three pedestals. Each data point is the mean of four threshold estimates, each obtained from a 300-trial psychometric function. Best-fitting straight lines have been drawn through each set of data. Because the data for the 0.01-contrast pedestal were collected over a narrower range of spectral densities, they are presented at increased scale in the insets.

Recall from the Introduction that, for targets of fixed size and duration, signal energy is proportional to squared contrast. For the Minnesota data, the conversion relation is $E = 0.0192C^2$ deg^2 sec. Using this conversion, the 0.01-contrast and 0.25-contrast pedestals have energies of 1.92 and 1200 μ(deg^2 sec), respectively. We can use the relation in reverse to convert threshold energies in Fig. 3 to threshold contrasts. For example, the no-noise, no-pedestal threshold energies for subjects DR and MK are 2.73 and 2.45 μ(deg^2 sec), respectively. These values convert to corresponding threshold contrasts of 0.0119 and 0.0113, respectively.

The results of the two observers are similar. First consider data points for zero noise spectral density. Thresholds for the 0.01-contrast pedestal lie below those for the zero-contrast pedestal (see insets). This is the facilitation effect in which near-threshold contrast discrimination is better than detection.[1] The corresponding threshold for the 0.25-contrast pedestal is much higher, representing the growth of increment threshold with suprathreshold pedestal contrast. It is interesting to compare our threshold signal energies with those measured by Watson *et al.*[34] They set out to find the target that could be detected with least signal energy (they used the term "contrast energy"). They found that a 7-c/deg sine wave drifting at 4 Hz, with Gaussian widths of 3 cycles in both the vertical and the horizontal directions and a duration of 160 msec, could be detected when its signal energy was about 1 μ(deg^2 sec). This is the target that "the eye sees best." [35] As computed in the previous paragraphs, in the absence of a pedestal our target required about 2.5 times more energy to be detected. However, when superimposed upon the 0.01-contrast pedestal, the threshold signal energy was about 0.7 μ(deg^2 sec), equivalent to or lower than

the signal energy in the stimulus of Watson *et al.* In an unpublished study, Kersten and Barlow[37] measured a substantially lower threshold energy [approximately 0.1 μ(deg^2 sec)] with a near-threshold pedestal added to the optimal stimulus found by Watson *et al.*

Recall that sampling efficiency is just the reciprocal of the slope k in Eq. (1). Notice that the slopes are about equal for the zero- and 0.01-contrast pedestals and for the two observers. However, the slope is about a factor of 2 lower for the 0.25-contrast pedestal for both observers. The drop in slope k implies an increase in sampling efficiency for discrimination at 0.25 contrast. The sampling efficiencies of both observers are plotted in Fig. 5A below. They are roughly 4% for detection and near-threshold discrimination and about 8% for suprathreshold contrast discrimination. (An efficiency of 8% means that, in high levels of noise, our observers' threshold signal energies were about 12 times greater than the ideal observer's threshold energy. This corresponds to threshold contrast about 3.5 times higher than the ideal.)

From Eq. (1), it can be seen that the intercept on the ordinate is equal to the product of k and N_{eq}. Therefore estimates of N_{eq} can be obtained by dividing the intercept by k. Values of N_{eq} are plotted in Fig. 5B. For the 0.01-contrast pedestal, values of N_{eq} have dropped by factors of 4.4 and 7.7 for subjects MK and DR, respectively. For the same condition, values of sampling efficiency have deviated by no more than 20% from those found for the zero-contrast pedestal. From these results, we conclude that the facilitation effect associated with near-threshold discrimination is due to a *reduction* in the observer's equivalent noise. On the other hand, for the 0.25-contrast pedestal, N_{eq} has risen by factors of 11.8 and 4.7 for subjects MK and DR, respectively, relative to values for the zero-contrast pedestal. At the same time, sampling efficiency has increased by a factor of about 2 for both observers. We may conclude that the growth of the increment threshold (intercept in Fig. 3) for suprathreshold pedestal contrasts is due to an *increase* in equivalent noise. Were it not for the small increase in sampling efficiency, the growth of equivalent noise would result in even larger increment thresholds. In short, the results of Fig. 3 indicate that the major features of the contrast-discrimination function can be traced to changes in the observer's equivalent noise.

An interesting aspect of the data in Fig. 3 is that the curves for zero- and 0.25-contrast pedestals cross. This means that, for high noise levels, observers can detect a smaller contrast increment superimposed upon a 0.25-contrast pedestal than upon a uniform background.

RESULTS: UNIVERSITY OF BRITISH COLUMBIA

The UBC results refer to contrast discrimination for 13.6-arcmin disks. Measurements were conducted with two-dimensional static noise. For the UBC data, the conversion relation between signal energy and contrast is $E = 0.0403C^2$ deg^2.

Figure 2B shows psychometric functions for two observers at a pedestal contrast of 0.053 and noise spectral density of 3.25 μ(deg^2). Each set of data is based on approximately 400 trials. Best-fitting straight lines (least-squares criterion)

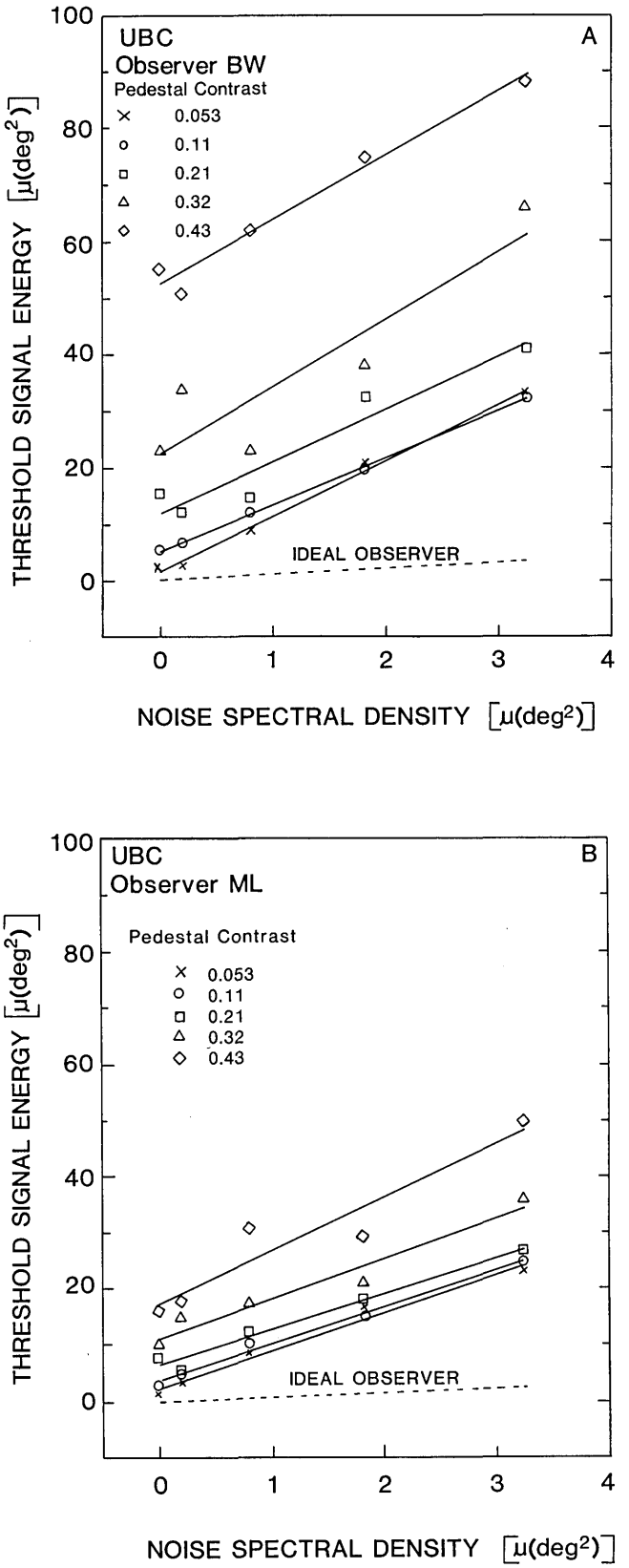

Fig. 4. Threshold signal energy as a function of noise spectral density in static noise (UBC). Data are shown for five pedestal contrasts ranging from 0.053 to 0.43. Best-fitting straight lines (least-squares criterion) have been fitted to the data. The dashed line with slope 1.0 shows the performance of an ideal observer. The relation between signal energy E and contrast C is $E = 0.0403C^2$ deg^2. A and B show data for two observers.

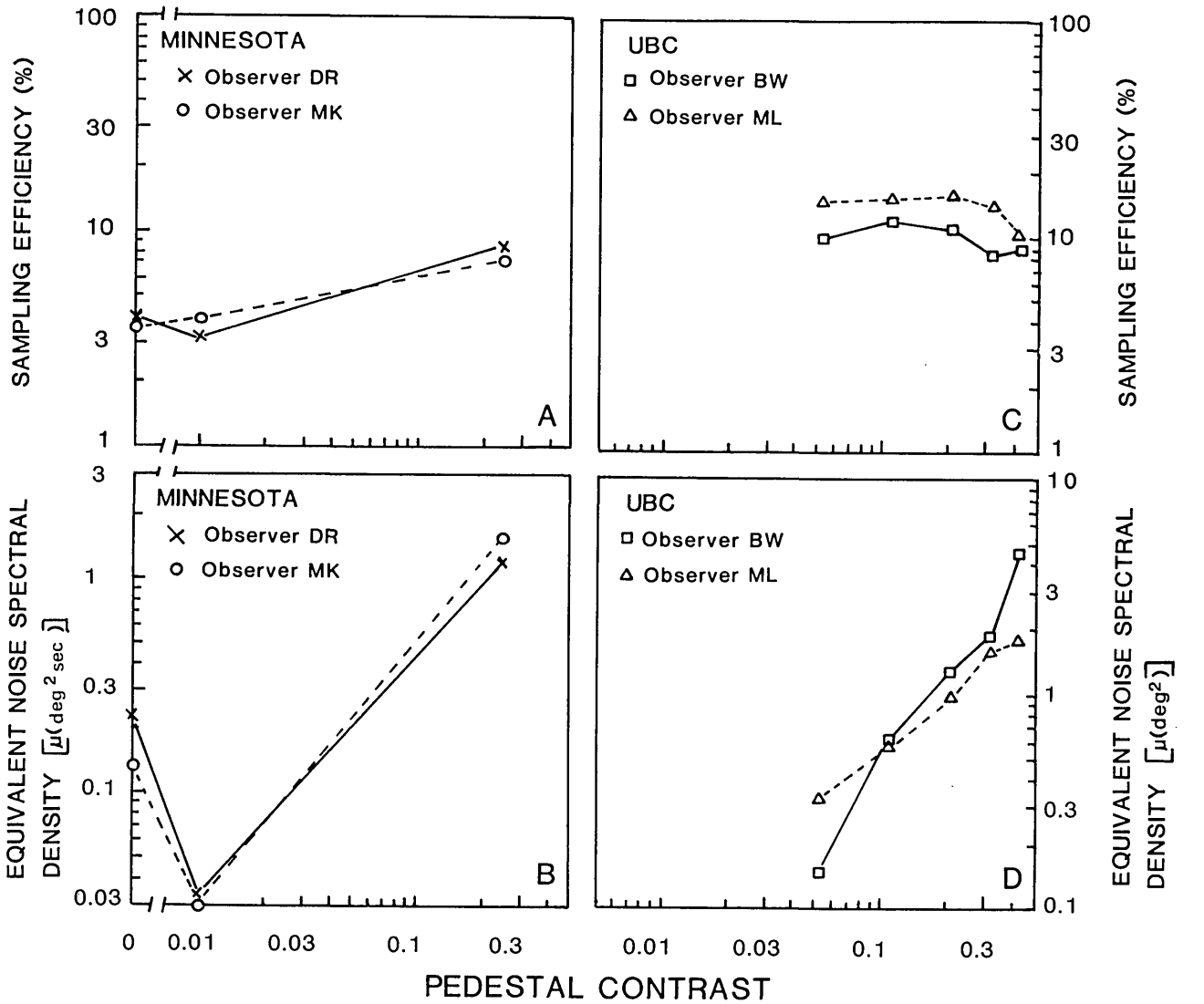

Fig. 5. Sampling efficiency and equivalent noise as a function of pedestal contrast. The values of sampling efficiency and equivalent noise that were estimated from the data of Figs. 3 and 4 are plotted for dynamic noise (panels A and B) and static noise (panels C and D).

through the two sets of data have slopes of 1.12 (subject ML) and 1.00 (subject BW). A slope near 1.0 in log–log coordinates implies a linear relationship between d' and increment contrast. The threshold is defined as the increment contrast for which $d' = 1$. In most cases, entire psychometric functions were not measured. Instead, percent correct (and hence d') was obtained for a single increment contrast. An assumed linear relationship between d' and increment contrast was then used to estimate the threshold. Linearity of psychometric functions for contrast discrimination in the presence or absence of static noise has been verified in numerous unpublished studies by A. E. Burgess. The example shown in Fig. 2B is for the lowest pedestal used in the UBC experiments. The Minnesota data in Table 1 indicate that as pedestal contrast or noise level increases, psychometric function slopes decrease to values near 1 and thereafter remain constant. None of the UBC data were collected for pedestal or noise levels in which nonlinear psychometric functions would be expected.

Figure 4 has the same format as Fig. 3. The two panels show data for observers BW and ML. Each point is based on 400 spatial forced-choice trials. Once again, the dashed curve with slope 1.0 shows the performance of an ideal observer. The five sets of data are for the five suprathreshold pedestal contrasts that ranged from 0.053 to 0.43. Lines were fitted to each set of data.

The leftmost data point in each set represents the increment threshold in the absence of noise. As expected, these values increase with increasing pedestal contrast. In fact, if the increment contrast is plotted as a function of pedestal contrast in log–log coordinates, the best-fitting straight lines through the data have slopes of 0.58 and 0.74 for subjcts ML and BW, respectively. This reflects existence of a power-law relation[38] between ΔC and C, in agreement with the findings of Legge[5] and Legge and Kersten.[6]

In each panel of Fig. 4, the sets of lines have very similar slopes. The corresponding sampling efficiencies for both observers are plotted in Fig. 5C. On the whole, subject ML's sampling efficiencies are about 1.4 times greater than subject BW's, roughly 14% compared with 10%. For both subjects, sampling efficiency remained relatively constant over the range of suprathreshold pedestals studied.

Values of N_{eq} can again be estimated by dividing the intercept on the ordinate by the corresponding value of k. These values are plotted in Fig. 5D. For both observers, N_{eq} rises monotonically with pedestal contrast. For subject BW, N_{eq} changes by a factor of about 32, whereas for subject ML, N_{eq} changes by a factor of only about 5.5. In less complete data for observer AB, not shown, N_{eq} increased by a factor of about 15 over the same range of contrasts. Despite these individual differences, it is clear that equivalent noise rises with pedestal contrast over the range examined.

In short, the UBC data reveal that, over the range of suprathreshold contrasts studied, sampling efficiency remains relatively constant, but equivalent noise rises with contrast. We therefore conclude that the growth of increment thresholds with suprathreshold pedestal contrast reflects the growth in the observer's equivalent noise.

DISCUSSION

Comparison of Findings in Static and Dynamic Noise

The results of experiments with static (UBC) and dynamic (Minnesota) noise have several common features. For both, a linear equation describes the relation between threshold signal energy and noise spectral density for contrast detection and discrimination. The two parameters of the linear equation are closely related to sampling efficiency and equivalent noise. Equivalent noise changes much more with pedestal contrast than sampling efficiency and therefore plays a greater role in determining the shape of the contrast-discrimination function. In dynamic noise, sampling efficiencies increased by only about a factor of 2 from no pedestal to a 0.25-contrast pedestal, whereas equivalent-noise spectral densities increased by factors of 5.2 and 11.9 for two subjects over the same range. In static noise, sampling efficiency showed no systematic variation across a log unit of suprathreshold pedestal contrast, whereas equivalent noise rose steadily in rough proportionality to pedestal contrast (Fig. 5D).

For suprathreshold pedestal contrasts, sampling efficiencies averaged 12 and 8% in static and dynamic noise, respectively. This near agreement may be somewhat fortuitous. It is likely that the Gaussian-windowed sine-wave signals used in the dynamic-noise experiments were more optimally matched to underlying detectors than were the disk signals used in the static-noise experiments. Had more nearly optimal stimuli been used in the latter, the static-noise sampling efficiencies would probably have been higher (cf. Burgess *et al.*[12]). Our results, therefore, do not conflict with the view that sampling efficiencies are higher in static than in dynamic noise.

The values of equivalent noise estimated in the static- and dynamic-noise experiments have different units and cannot therefore be directly compared. However, we briefly digress to compare the values of equivalent noise in the dynamic experiments with values to be expected if the photon flux were the only intrinsic source of noise. The retinal illuminance corresponding to 340 cd/m^2 and a measured pupil diameter of 5 mm is 6675 Td. Since one troland corresponds to 1.25×10^6 photons per deg^2 sec at 555 nm, the total photon flux, for two eyes, was 1.67×10^{10} photons per deg^2 sec. The reciprocal of the photon flux is the noise spectral density, and, in this case, it is equal to 5.99×10^{-5} μ(deg^2 sec). By comparison, subject MK's measured value of equivalent noise for detection with no pedestal was 0.135 μ(deg^2 sec). The ratio of photon-noise spectral density to subject MK's equivalent-noise spectral density is 4.44×10^{-4}. Pelli[11] has termed such a ratio the observer's "transduction efficiency." Pelli has shown that quantum efficiency is the product of transduction efficiency and sampling efficiency. Since subject MK's sampling efficiency is 4% for detection, her quantum efficiency is 0.0017%.

Implications for Models of Contrast Discrimination

Two aspects of the contrast-discrimination function have attracted theoretical interest—the facilitation effect and the growth of increment threshold with suprathreshold pedestal contrast. We treat these separately.

Facilitation Effect

Why does threshold increment contrast decrease as pedestal contrast increases from zero? For theoretical analyses, see papers by Foley and Legge,[4] Wilson,[8] Lasley and Cohn,[39] and Pelli.[24] Of the models to be reviewed, only the *threshold-transducer* model accounts for the data of this paper.

A leading theoretical candidate is the *signal-uncertainty model*, one version of which has been described in detail by Pelli.[24] According to this model, an observer monitors the output of M linear, independent noisy detectors, only one of which (or possibly several of which) is responsive to a given signal. All M detectors, however, are assumed to be equally responsive to white noise. In a two-alternative forced-choice (2AFC) trial, the observer adopts a maximum-of-decision rule; he chooses the alternative in which he finds the detector yielding the largest output.[40] When such an observer attempts to detect a signal in the absence of a pedestal, noise in the nonsignal channels causes the threshold to rise relative to an ideal observer, who ignores the noise from the nonsignal channels. In the terminology of this paper, the signal-uncertain observer is oversampling; he gathers information from an inappropriately large set of detectors. Equations governing the behavior of this model for detection have been presented by Nolte and Jaarsma[41] and by Pelli.[11,24] Pelli has also presented an equation and a graph describing performance of the model for discrimination.

How does the uncertainty model behave for contrast discrimination? Because the pedestal and increment are identical except for amplitude, both stimulate the signal-sensitive detector. In the 2AFC procedure, the observer once again monitors all M detectors in both alternatives and selects the alternative in which he finds the detector having maximum response. The model exhibits different behavior, depending on whether the pedestal itself is subthreshold or suprathreshold. By definition, when the pedestal is subthreshold, its detectability is low. This means that its presence does not much increase the odds that the signal-sensitive detector will carry the maximum response. The situation remains much like detection in which the noise from the $M - 1$ nonsignal detectors reduces efficiency. On the other hand, when the pedestal is suprathreshold, its detectability is high. This means that its presence will usually guarantee that the maximum response will arise from the signal-sensitive detector. As a consequence, the effect of uncertainty diminishes, even though the observer continues to monitor

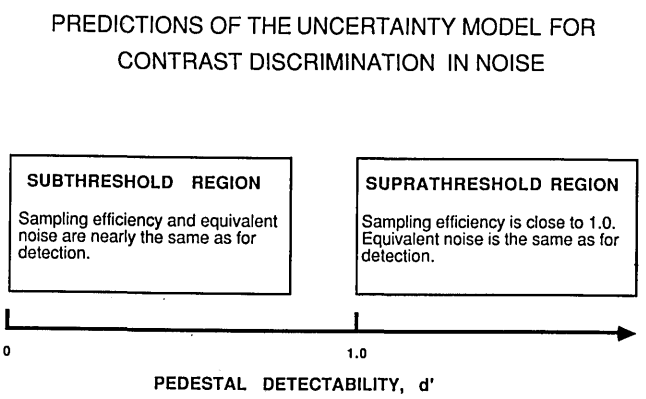

Fig. 6. Summary of the properties of the signal-uncertainty model for discrimination in noise. The model's behavior depends on the detectability d' of the pedestal. For details, see the text.

all M detectors. When the pedestal acts in this way to reduce the effect of uncertainty, the increment threshold is lower. This is the model's explanation for the facilitation effect. When the pedestal contrast is high enough so that the forced-choice decision is always based on the output of the signal-sensitive channel, the increment threshold drops to the value achieved by an ideal observer, who monitors only the signal-sensitive detector. In short, a suprathreshold pedestal causes a signal-uncertain observer to perform as well as the $M = 1$ ideal observer.

The analysis is the same when external noise is added, except that the subthreshold and suprathreshold domains of behavior are defined by the detectability of the pedestal in the external noise. If the range of noise levels is low enough so that the pedestal remains well above threshold, the model's discrimination behavior is nearly ideal, and the sampling efficiency is close to 1. If the external noise levels are so high that the pedestal has extremely low detectability, the model's discrimination behavior is much like its detection behavior, so sampling efficiency is lower. In these two domains, linear equations provide good descriptions of performance. The two types of behavior can be modeled by curves A and C in Fig. 1. For both, the estimated value of equivalent noise is the same (X-axis intercept). When the pedestal is suprathreshold, the slope is unity (curve A), corresponding to a sampling efficiency of 1. When the pedestal is subthreshold, the slope is higher (curve C), corresponding to a lower sampling efficiency. This illustrates that a single decision rule can exhibit different sampling efficiencies, depending on its domain of application. Finally, if a set of noise levels covers a range in which the pedestal is sometimes subthreshold and sometimes suprathreshold, hybrid performance will result. For low noise levels, the data will lie along curve A; for high noise levels, along curve C. The transition occurs when the noise levels are such that the pedestal has detectability d' near 1. Taken as a whole, the hybrid curve is nonlinear. Straight-line fits across the transitional region would provide spuriously low estimates of both sampling efficiency and equivalent noise. Figure 6 summarizes the uncertainty model's discrimination behavior. If the pedestal itself is suprathreshold, $d' > 1$, then discrimination performance is nearly ideal. If the pedestal is subthreshold, $d' < 1$, discrimination is much like detection.

The uncertainty model predicts that sampling efficiency should be higher for data collected with suprathreshold pedestals than for data collected with subthreshold pedestals. To test this prediction for a given pedestal would require a range of noise levels great enough so that the pedestal itself was sometimes subthreshold and sometimes suprathreshold. Unfortunately, none of our data sets was of this type. Our near-threshold pedestal had a contrast of 0.01, and subjects DR and MK had detection thresholds of 0.0113 and 0.0119, respectively. This means that the detectability of the pedestal, in the absence of external noise, was already lower than 1. (In fact, we may use the slopes of the psychometric functions listed in the top row of Table 1 to estimate that the pedestal had detectabilities of 0.70 and 0.77 for subjects DR and MK, respectively.) Addition of external noise would lower the d' values still further. These conditions are appropriate for the subthreshold region in Fig. 6. On the other hand, our higher-contrast pedestals were all confined to the suprathreshold region in Fig. 6.

We conducted a supplementary experiment to test the uncertainty model. Apparatus, procedures, and stimulus waveforms were the same as described in the Minnesota Method section. Subject MK participated in the supplementary experiment that was conducted two years after the original experiments. Contrast discrimination was measured for a 0.024-contrast pedestal. Preliminary measurements indicated that this target by itself had detectability of 1 when the noise spectral density was 0.177 $\mu(\text{deg}^2\ \text{sec})$. Using this pedestal, we measured subject MK's contrast-increment thresholds for noise levels lower than 0.177 (suprathreshold region) and for noise levels greater than 0.177 (subthreshold region). The results are shown in the two panels of Fig. 7. Data for the subthreshold pedestal are shown in Fig. 7A and for the suprathreshold pedestal in Fig. 7B. The uncertainty model predicts that the slope of the best-fitting straight line will be greater in Fig. 7A than in Fig. 7B. Indeed, the slope is slightly higher for the subthreshold pedestal, but not significantly so—23.2 ± 3.98, compared with 15.6 ± 5.21. These data do not provide evidence for a major change in slope. Recall that sampling efficiency is the reciprocal of these slopes. The values are 4.3% (subthreshold pedestal) and 6.4% (suprathreshold pedestal), similar to the earlier estimates for subject MK (Fig. 5A). These data do not confirm the uncertainty model's prediction that the sampling efficiency should be higher for contrast discrimination when the pedestal is suprathreshold than when it is subthreshold.

Our data pose an additional problem for the uncertainty model. The model predicts that the slopes of detection psychometric functions should be the same in the presence or absence of external noise. As Table 1 shows, we found lower slopes for detection in noise than for detection in the absence of noise.

In summary, our results do not appear to support an interpretation of the facilitation effect based on signal uncertainty. It should be noted, however, that a more thorough quantitative test of the model awaits specific proposals for the value of M and for the range of conditions over which the model applies.

Legge[42] has shown that an energy-detector model can account for several aspects of contrast detection and discrimination, including the facilitation effect. According to this model, intrinsic Gaussian noise is added to the signal, bandpass filtered, squared, and integrated. (At suprathreshold

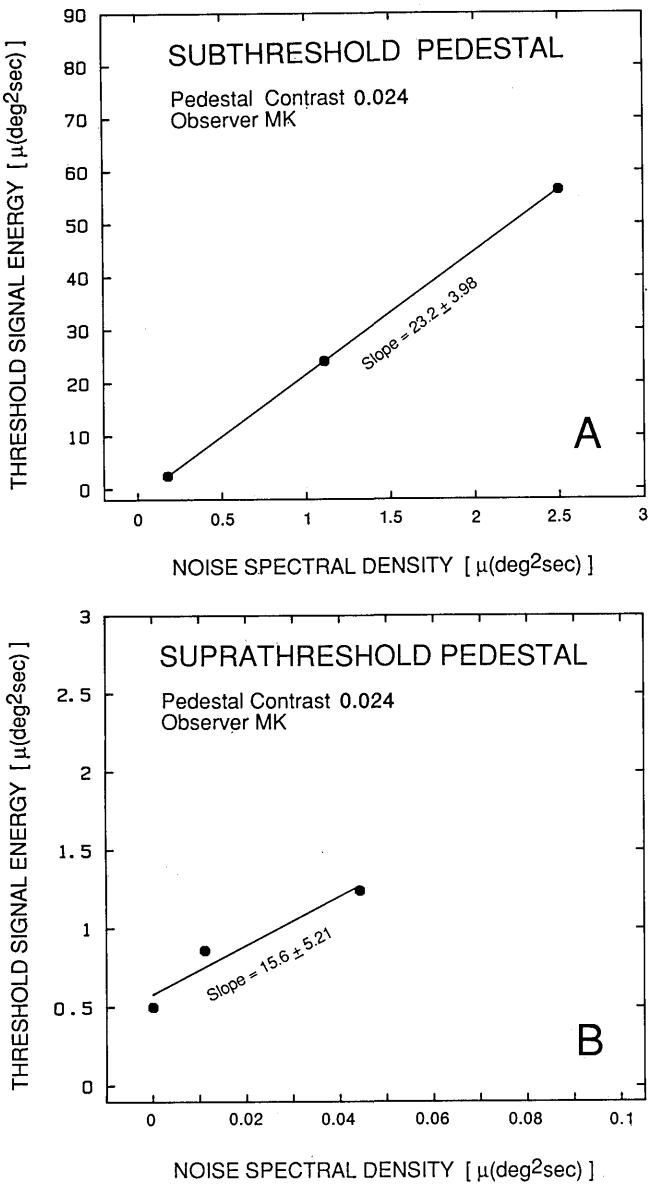

Fig. 7. Threshold signal energy as a function of noise spectral density in dynamic noise (Minnesota). In these experiments, the pedestal had a contrast of 0.024 with corresponding signal energy of 11 $\mu(\text{deg}^2\,\text{sec})$. For observer MK, its detectability d' is 1 for a noise spectral density of 0.177 $\mu(\text{deg}^2\,\text{sec})$. Panel A shows threshold signal energy for contrast increments when noise levels are higher than this, and panel B shows that for lower noise levels. Each point is the mean of four threshold estimates, each based on a 300-trial psychometric function. Best-fitting straight lines (least-squares criterion) have been fitted to the data.

contrasts, a compressive nonlinearity also plays a role. See the next subsection.) The type of square-law summation inherent in this model is nonideal when it comes to the detection of known signals. Accordingly, the sampling efficiency of the energy detector decreases with the spatiotemporal extent of the signal, as characterized by the number M of spatial and temporal samples required to represent it. We studied the properties of this model for contrast detection and discrimination in noise. The results can be summarized by saying that the energy detector behaves qualitatively like the signal-uncertainty model. Once again, the model behaves differently for subthreshold and suprathreshold pedestals, with higher sampling efficiency in the latter. The empirical arguments marshalled against the signal-uncertainty model once again apply. Therefore our results do not support an interpretation of the facilitation effect based on the energy detector.

Laming[43] has developed a comprehensive model of sensory processing that includes contrast detection and discrimination. The only source of noise in the model is the photon flux. Because of its Poisson nature, the mean and the variance of the flux are both proportional to luminance. There is a stage of exact differential coupling at the input. It transforms the photon flux to a source of noise (approximately Gaussian in form at photopic levels), with zero mean and variance proportional to luminance. Subsequently, there is a stage of half-wave rectification followed by integration. For small signals, the output is an accelerating function of input amplitude. This property accounts for the form of the detection psychometric function and for the facilitation effect. According to this model, presentation of zero-mean, constant-variance, Gaussian white noise before the stage of differential coupling is equivalent to the addition of a uniform veiling luminance. We can predict the effects of a veiling luminance on contrast detection as follows. At moderate and high levels of illumination, Weber's law applies, and contrast-detection thresholds are independent of background luminance L_0. Addition of a veiling luminance L_v would result in an apparent increase in threshold by a factor of $1 + (L_v/L_0)$ and an increase in threshold signal energy by a factor of $[1 + (L_v/L_0)]^2$. According to Laming's model, noise spectral density N is equivalent to veiling luminance L_v, so we should expect a quadratic relation between threshold signal energy and N. This prediction disagrees with the present study and with a variety of other studies that have shown a linear relation and not a quadratic one. A similar analysis indicates that the relation between squared increment contrast and veiling luminance is also nonlinear, implying that Laming's model predicts a nonlinear relation between threshold signal energy and noise spectral density. This again is inconsistent with our data.

Foley and Legge[4] studied the form of psychometric functions for contrast detection and near-threshold discrimination. They proposed a *threshold-transducer model* to account for their data. According to their model, a response proportional to stimulus amplitude is perturbed by a source of peripheral noise (possibly quantal in origin) and is then subjected to a thresholding operation. If the response exceeds a threshold value T, it is unaffected. If the response is less than T, it is set to zero. The level of T is set so that fluctuations of the peripheral-noise source rarely exceed it in the absence of a signal. Following the thresholding operation, the response is perturbed by a central source of noise that is independent of the peripheral source. Unlike the signal-uncertainty and energy-detector models, the threshold-transducer model contains just one channel. Its performance is determined in large part by the *central* noise that *follows* the nonlinearity.

We used a Monte Carlo simulation to study the properties of the threshold-transducer model for detection and discrimination in noise. To do so, it was necessary to assign values to the threshold T, the peripheral-noise standard deviation, and the central-noise standard deviation. A lim-

ited search of the parameter space revealed that values of 3.0, 1.0, and 1.25, respectively, provided satisfactory results. For a given pedestal and noise level, threshold contrast was estimated from a simulated psychometric function composed of four to six noise levels and 500 trials per level. Threshold signal energy was computed from squared threshold contrast and plotted as a function of noise spectral density. The simulation produced the following results. (1) The detection psychometric function had the form d' proportional to $C^{2.7}$. (2) The increment threshold for a near-threshold pedestal was about a factor of 2 lower than the detection threshold. (3) For both detection and discrimination, threshold signal energy was linearly related to noise spectral density. (4) In high noise, psychometric functions for detection and discrimination were both approximately linear, that is, d' proportional to C. (5) Relative to detection, the sampling efficiency for near-threshold discrimination, changed by no more than 12%, whereas the equivalent noise dropped by a factor of 4. All these properties are consistent with the data presented in this paper and with the relevant data of Foley and Legge.[4]

Of the models considered here for detection and near-threshold discrimination, only the threshold-transducer model is consistent with our data.

Suprathreshold Contrast Discrimination

Several models have been proposed to account for the suprathreshold behavior of contrast discrimination.[3,8,9,42,44] These models account for the growth of the increment threshold in one of two ways. Either there is a compressive transformation of internal response followed by the addition of a constant-variance noise or there is a linear response to which is added signal-dependent (multiplicative) noise. The form of the compressive nonlinearity or the relation between signal strength and noise variance is manipulated to account for discrimination data. There exists electrophysiological evidence for signal-dependent noise. Tolhurst *et al.*[45] measured the mean and the standard deviation of the number of spikes elicited by passage of 1 cycle of a drifting grating through the receptive fields of 20 cat simple and complex cells. Over a range of contrasts between threshold and saturation, the standard deviation increased as a power function of the mean with exponent in the range 0.5–0.7.

It would be nice if our noise experiments could distinguish between these two types of models. Unfortunately, they cannot. In fact, as is shown in Appendix A, it is unlikely that psychophysical discrimination experiments can distinguish between the two alternatives. Both types of model predict that sampling efficiency remains constant as pedestal contrast rises but that equivalent noise increases. This prediction is fully consistent with our static-noise data (Fig. 4). Our dynamic-noise data (Fig. 3) show an increase by a factor of 2 in sampling efficiency from near-threshold to suprathreshold pedestals. The reason for this change in sampling efficiency is not known.

Whereas our noise results were inconsistent with most models of near-threshold contrast coding, they tend to support the prevailing view of suprathreshold contrast discrimination.

Models such as those just described for suprathreshold contrast discrimination have also been used to account for Weber's law for luminance discrimination. Such models would predict that sampling efficiency remains constant and equivalent noise grows as luminance increases. However, Pelli[46] has analyzed data showing that sampling efficiency must drop dramatically as luminance increases. Pelli's analysis implies that the Weber's law for luminance discrimination results not from nonlinear compression or signal-dependent noise but from decreasing sampling efficiency.

In summary, our experimental results appear to be inconsistent with most models of contrast coding near the detection threshold. Our data do not support Pelli's[24] uncertainty model, Legge's[42] energy detection model, or Laming's[43] rectifier–integrator model. They do support Foley and Legge's[4] threshold-transducer model. Our suprathreshold discrimination results are, in general, consistent with existing models. Our suprathreshold data indicate that the growth of the contrast-increment threshold is due to the growth of equivalent noise, not to a decrease in sampling efficiency.

APPENDIX A: PSYCHOPHYSICAL EQUIVALENCE OF TWO MODELS OF CONTRAST CODING

We show that, for suprathreshold psychophysical discrimination, a compressive nonlinearity followed by invariant noise is equivalent to a linear response perturbed by signal-dependent noise.

Suppose that a stimulus with amplitude A is added to an external source of Gaussian noise having zero mean and variance S_1^2. To this we add a source of intrinsic peripheral noise (perhaps quantal or neural in origin) with zero mean and variance S_2^2. The corresponding internal response is a Gaussian random variable with mean A and variance $S_1^2 + S_2^2$. This variable is subjected to a compressive transformation $F(x)$. Proposals for the form of $F(x)$ range from log to power laws with exponent less than unity. We can represent $F(x)$ by a Taylor-series expansion about some fixed value of x. The fixed value of x corresponds to a particular stimulus amplitude, say, A_0. The expansion is

$$F(x) = F(A_0) + F'(A_0)(x - A_0) + F''(A_0)(x - A_0)^2 + \ldots .$$

For most cases of suprathreshold discrimination, x and A_0 are similar, that is, pedestal and pedestal-plus-signal amplitudes do not differ by much. Therefore $(x - A_0)$ is small, and the squared and higher terms can be neglected. By doing so, we are assuming that the amplitudes under study within a given analysis are sufficiently close together so that the nonlinearity can be approximated by a linear function with slope equal to the derivative of the nonlinearity for the amplitude in question. Therefore

$$F(x) \approx gx + b,$$

where $g = F'(A_0)$ and is termed the "differential gain," and $b = F(A_0) - F'(A_0)A_0$. When our Gaussian random variable passes through this transformation, its mean becomes $gA + b$ and its variance becomes $g^2(S_1^2 + S_2^2)$. To this variable is added central noise with zero mean and variance S_3^2. Therefore the decision variable has mean $gA + b$ and variance $g^2(S_1^2 + S_2^2) + S_3^2$ for signals with amplitudes near A_0. Suppose that the observer is required to discriminate be-

tween signals having amplitudes of A_0 and A_1, both presented in the same source of external noise. The proportion correct in forced choice is determined by the difference distribution of the decision variables associated with the two stimuli. The mean of this distribution is $g(A_1 - A_0)$. Its variance is $2[g^2(S_1^2 + S_2^2) + S_3^2]$. The proportion correct depends only on the ratio of mean to standard deviation. This ratio is equal to $(A_1 - A_0)/2^{1/2}[S_1^2 + S_2^2 + (S_3/g)^2]^{1/2}$. This is exactly the same ratio that would result if a linear response function were perturbed by internal noise with variance $S_2^2 + (S_3/g)^2$, that is, internal noise that depends on the differential gain g. Since g is the derivative of the compressive transformation, it gets smaller as pedestal amplitude A_0 increases. Therefore the equivalent-noise variance $S_2^2 + (S_3/g)^2$ rises.

This analysis shows the equivalence of a compressive nonlinearity to an internal, signal-dependent source of noise. Both can be characterized by changes in the observer's *equivalent noise.*

ACKNOWLEDGMENTS

The Minnesota research was supported by U.S. Public Health Service grant EY02857 to Gordon E. Legge. The UBC research was supported by Medical Research Council of Canada grant MA-7621 to Arthur E. Burgess. We thank Maureen Karpan, Holli Rietmulder, Traci Toomey, and Mary Schleske for help with manuscript preparation; Yuanchao Gu for help in running the supplementary experiment; and Gary Rubin and Donald Laming for comments on a draft. We thank Denis Pelli for comments on several drafts and for a great deal of useful discussion, particularly concerning the uncertainty model.

REFERENCES AND NOTES

1. J. Nachmias and R. V. Sansbury, "Grating contrast: discrimination may be better than detection," Vision Res. **14,** 1039–1042 (1974).
2. C. F. Stromeyer III and S. Klein, "Spatial frequency channels in human vision as asymmetric (edge) mechanisms," Vision Res. **14,** 1409–1420 (1974).
3. G. E. Legge and J. M. Foley, "Contrast masking in human vision," J. Opt. Soc. Am. **70,** 1458–1471 (1980).
4. J. M. Foley and G. E. Legge, "Contrast detection and near-threshold discrimination in human vision," Vision Res. **21,** 1041–1053 (1981).
5. G. E. Legge, "A power law for contrast discrimination," Vision Res. **21,** 457–467 (1981).
6. G. E. Legge and D. Kersten, "Light and dark bars: contrast discrimination," Vision Res. **23,** 473–483 (1983).
7. G. E. Legge, "Spatial frequency masking in human vision: binocular interactions," J. Opt. Soc. Am. **69,** 838–847 (1979).
8. H. R. Wilson, "A transducer function for threshold and suprathreshold spatial vision," Biol. Cyb. **38,** 171–178 (1980).
9. G. J. Burton, "Contrast discrimination by the human visual system," Biol. Cyb. **40,** 27–38 (1981).
10. H. B. Barlow, "Retinal and central factors in human vision limited by noise," in *Vertebrate Photoreception,* H. B. Barlow and P. Fatt, eds. (Academic, New York, 1977).
11. D. G. Pelli, "The effects of visual noise," Ph.D. dissertation (Department of Physiology, Cambridge University, Cambridge, UK, 1981).
12. A. E. Burgess, R. F. Wagner, R. J. Jennings, and H. B. Barlow, "Efficiency of human visual signal discrimination," Science **214,** 93–94 (1981).
13. In the absence of a pedestal, when $L_p = L_0$, $S(x, y, t)$ is sometimes termed a *contrast function.*[14]
14. E. H. Linfoot, *Fourier Methods in Optical Image Evaluation* (Focal, New York, 1964).
15. N. S. Nagaraja, "Effect of luminance noise on contrast thresholds," J. Opt. Soc. Am. **54,** 950–955 (1964).
16. Pelli[11] wrote Eq. (1) with k expressed as $(d'_c{}^2/J)$, as presented in Eq. (3). He used the term "calculation efficiency" for J rather than "sampling efficiency." Nagaraja[15] used "squared normalized luminance" rather than "signal energy" and "variance" rather than "spectral density" having absorbed several values into k.
17. W. A. Wickelgren, "Unidimensional strength theory and component analysis of noise in absolute and comparative judgments," J. Math. Psychol. **5,** 102–122 (1968).
18. W. P. Tanner, Jr., and T. G. Birdsall, "Definitions of d' and η as psychophysical measures," J. Acoust. Soc. Am. **30,** 922–928 (1958).
19. A. E. Burgess and H. B. Barlow, "The precision of numerosity discrimination in arrays of random dots," Vision Res. **23,** 811–820 (1983).
20. D. Kersten, "Spatial summation in visual noise," Vision Res. **24,** 1977–1990 (1984).
21. D. Kersten and H. B. Barlow, "Searching for the high-contrast patterns we see best," Suppl. Invest. Ophthalmol. Vis. Sci. **25,** 313 (1984).
22. D. Kersten and H. B. Barlow, "Why are contrast thresholds so high?" Suppl. Invest. Ophthalmol. Vis. Sci. **26,** 140 (1985).
23. When the analysis is done in time and two spatial dimensions, the stochastic nature of the photon flux adds noise to the stimulus. If this noise is not included as part of the external noise N, it will appear as a nonzero value of equivalent noise for the ideal observer. Pelli[11] has pointed out that the photon-noise spectral density is equal to the reciprocal of the photon flux.
24. D. G. Pelli, "Uncertainty explains many aspects of visual contrast detection and discrimination," J. Opt. Soc. Am. A **2,** 1508–1532 (1985).
25. F. W. Campbell and D. G. Green, "Optical and retinal factors affecting visual resolution," J. Physiol. (London) **181,** 576–593 (1965).
26. P. Horowitz and W. Hill, *The Art of Electronics* (Cambridge U. Press, Cambridge, 1980).
27. The rapid decay of the P31 phosphor—the intensity drops to 1% within 250 μsec (Ref. 28)—is very short compared with the integration time of the eye. Therefore the 100-Hz frame rate of the display determines the temporal sampling characteristics relevant to the calculation of noise spectral density.
28. R. A. Bell, "Principles of cathode-ray tubes, phosphors and high-speed oscillography," Hewlett-Packard Application Note 115 (Hewlett-Packard, Colorado Springs, Colo., 1970).
29. We derive this for one dimension. The three-dimensional case is a straightforward extension. We need to show that, in one dimension, the contrast power spectral density for pixel noise is

$$N(f) = bc_{\text{rms}}{}^2 \operatorname{sinc}^2(bf), \tag{R1}$$

where b is the extent of the pixel (in degrees or seconds), $c_{\text{rms}}{}^2$ is the contrast power, and f is the frequency (in cycles per degree or hertz). Consider a contrast noise sample of 1-sec duration:

$$c(t) = \sum_{n=0}^{(1/b)-1} c(nb)\ \text{rect}\left(\frac{t - nb}{b}\right).$$

By averaging the squared modulus of the Fourier transform of $c(t)$, we get

$$\overline{C(f)C^*(f)} = b^2 \operatorname{sinc}^2(bf) \sum_{n=0}^{(1/b)-1} \overline{c^2(nb)},$$

where we have assumed that adjacent pixel contrasts are uncorrelated. Further, assuming stationarity,

$$N(f) = b^2 \operatorname{sinc}^2(bf) c_{\text{rms}}{}^2 1/b = b \operatorname{sinc}^2(bf) c_{\text{rms}}{}^2,$$

which is Eq. (R1). The signals in our experiments were at low spatiotemporal frequencies relative to the first zero of $N(f)$, which occurs at $f = 1/b$ (118 c/deg, 12 c/deg, and 100 Hz for the horizontal, vertical, and temporal frequencies). Thus the spec-

tral density is approximately flat in the region of the signals and is given by

$$N(f) = N(0) = c_{\text{rms}}{}^2 b$$

or, in three dimensions, by

$$c_{\text{rms}}{}^2 b_x b_y b_t,$$

where b_x, b_y, and b_t are the horizontal, vertical, and temporal sample sizes, respectively.

30. D. M. Green and J. A. Swets, *Signal Detection Theory and Psychophysics* (Krieger, Huntington, N.Y., 1974).
31. The quantization of the gray levels contributes additional noise. If we assume that the probabilities of the gray levels from the noise process are uniformly distributed across a quantization step, the quantization variance is $Q^2/12$ per pixel, where Q is the gray-level step size.[32] The noise spectral density equals rms contrast squared × pixel width × pixel height equals $(1/128)^2 \times (0.014)^2 \times (1/12)$ equals 0.001 $\mu(\text{deg}^2)$, which is negligible compared with the externally added noise.
32. A. Burgess, "Effect of quantization noise on visual signal detection in noisy images," J. Opt. Soc. Am. A **2,** 1424–1428 (1985).
33. W. L. Hays, *Statistics for Psychologists* (Holt, New York, 1963).
34. A. B. Watson, H. B. Barlow, and J. G. Robson, "What does the eye see best?" Nature **302,** 419–422 (1983).
35. The photopic quantum efficiencies found for intensity detection and discrimination of point sources[36] are much higher (about 5%) than that of the optimal stimulus of Watson *et al.*[34] (about 0.05%). However, a comparison in terms of contrast energy is problematic because contrast energy is not well defined for a point source.
36. W. S. Geisler and K. D. Davila, "Ideal discriminators in spatial vision: two-point stimuli," J. Opt. Soc. Am. A **2,** 1483–1497 (1985).
37. D. Kersten, Department of Psychology, Brown University, Providence, R.I. 02912, and H. B. Barlow, Department of Physiology, Cambridge University, Cambridge CB2 3EG, UK (personal communication).
38. For disks superimposed upon a uniform background, there is a nonlinear relationship between contrast defined as $\delta L/L$ and Michelson contrast, $(L_{\text{max}} - L_{\text{min}})/(L_{\text{max}} + L_{\text{min}})$. The slopes cited in the text were calculated with contrast defined in the former way. The corresponding slopes for Michelson contrast are 0.45 and 0.62. The issue of contrast definition is dealt with in more detail by Legge and Kersten.[6]
39. D. J. Lasley and T. E. Cohn, "Why luminance discrimination may be better than detection," Vision Res. **21,** 273–278 (1981).
40. The maximum-of-M-channels decision rule differs from the ideal decision rule for detection by a signal-uncertain observer.[41] However, it is computationally simpler than the ideal rule and closely approximates it. For further discussion, see Pelli.[24]
41. L. W. Nolte and D. Jaarsma, "More on the detection of one of M orthogonal signals," J. Acoust. Soc. Am. **41,** 497–505 (1967).
42. G. E. Legge, "Binocular contrast summation—II. Quadratic summation," Vision Res. **24,** 385–394 (1984).
43. D. Laming, *Sensory Analysis* (Academic, New York, 1986).
44. C. Carlson and R. Cohen, "A nonlinear spatial frequency signal detection model for the human visual system," J. Opt. Soc. Am. **68,** 1379 (1978).
45. D. J. Tolhurst, J. A. Movshon, and I. D. Thompson, "The dependence of response amplitude and variance of cat visual cortical neurons on stimulus contrast," Exp. Brain Res. **41,** 414–419 (1981).
46. D. G. Pelli, "The transduction efficiency of human vision," Suppl. Invest. Ophthalmol. Vis. Sci. **21,** 48 (1982).